Journal of Zhejiang University SCIENCE A
ISSN 1673-565X (Print); ISSN 1862-1775 (Online)
www.zju.edu.cn/jzus; www.springerlink.com
E-mail: jzus@zju.edu.cn

Simulation and analysis of resin flow in injection machine screw*

Ling-feng LI†[1], Samir MEKID[2]

([1]*College of Mechanical and Energy Engineering, Zhejiang University, Hangzhou 310027, China*)

([2]*School of Mechanical, Aerospace and Civil Engineering, University of Manchester, Manchester, UK*)

†E-mail: melilf@zju.edu.cn

Received Sept. 10, 2007; revision accepted Nov. 1, 2007; published online Jan. 18, 2008

Abstract: A method with simulation and analysis of the resin flow in a screw is presented to ease the control of some problems that may affect the efficiency and the quality of the product among existing screws in an injection machine. The physical model of a screw is established to represent the stress, the strain, the relationship between velocity and stress, and the temperature of the cells. In this paper, a working case is considered where the velocity and the temperature distributions at any section of the flow are obtained. The analysis of the computational results shows an ability to master various parameters depending on the specifications.

Key words: Screw, Plasticity, Velocity distribution, Temperature distribution
doi:10.1631/jzus.A071471 **Document code:** A **CLC number:** TH12

INTRODUCTION

In plastic industrial production, about 80% resin is processed by screw-barrel plasticity and most pre-processes which include transport, dehydration and drain employ plasticity. The screw plays an important role in a plastic injection machine. It is a crucial component in injection machine and its performance has a huge impact on the production and the quality of the product.

The high performance computer hardware and sophisticated software make it possible to study industrial polymer processed by numerical computation (Mackerle, 2003; Shojaei, 2006). Finite element method (FEM) is widely used to help us understanding the complicated physical phenomena in material processing situations where nonlinear interactions have to be taken into account (Shojaei *et al*., 2004).

Even though the material properties may sometimes be simulated experimentally, part of the polymer process can be numerically simulated by the FEM in an efficient and low-cost way (Cheung *et al*., 2004; Savarmand *et al*., 2007; Das *et al*., 2006). In numerical simulation, analyses of the mixing of polymer melts are helpful in determining the overall average progression of dispersion (Ghoreishy *et al*., 2005; Kessels *et al*., 2007). A mixed low-order finite element technique has been developed for the analysis of 2D viscoelastic flows in the presence of multiple relaxation time (Bogaerds *et al*., 1999). The distribution of velocity and stress components, temperature and pressure fields can be obtained by 2D approximations.

A simple model to describe the low-density polyethylene and polystyrene (LDPE/PS) compounded in a single-screw extruder has been proposed (Wilczyñski *et al*., 2001). The model calculates the mass flow rate of polymer pressure and temperature profiles along the extruder screw channel. However, it cannot give the detailed value of a point in a section across the channel.

The injection molding process involves filling, packing and holding and solidifying, but computer simulations in most papers have concentrated on the filling stage (Bogaerds *et al*., 2004). The phenomena in the channel of screw are seldom investigated.

Plasticity includes a series of elementary pro-

* Project supported by the National Natural Science Foundation of China (No. 10476026) and the Natural Science Foundation of Zhejiang Province (No. Y106655), China

cedures that happen between the screw and the barrel, such as solid transportation, gaining pressure, blending, exhaust and pumping (Lerdwijitjarud *et al*., 2004; Russo and Zuccarello, 2007). However, there are still a few problems that negatively affect the efficiency and quality of product among existing screws. One of the problems is that the resin generates redundant shearing heat that results in temperature overrun and resin decomposition while processing. Another problem is related to high speed. The screw works in a poor way when the rotation speed of screw reaches a high value. Further problem comes forth while abundance of new material with high stickiness is applied in practice, because some screws are not adapted to new resin processing (Zampaloni *et al*., 2007). Table 1 gives an exergue of common problems with possible causes. The temperature effect is one of the repeatable causes in most common problems experienced with various machines.

Solving these problems and improving the performance of the screw is a tremendously hard task on account of complexity of the plasticity, multi-disciplinary aspects and mutual effect of many factors. Regarding the plasticity process and since it is only three decades after the physical phenomenon that happened in the screw was understood, many others are not clearly known (Wilczyñski, 2001). The disciplines related to plasticity process include solid mechanics, hydromechanics, heat exchange, macromolecule physics, and rheology (Restrepo *et al*., 2007). Because of a large number of variable process parameters, material characteristic parameters of polymer and operating conditions, it is difficult to get an exact quantitative equation to describe the screw performance (Hasanpour and Ziaei-Rad, 2007; Ekh and Schön, 2008; Lesniak and Libura, 2007).

In this paper, numerical simulation and analysis of the plastic material flow in a screw are used to observe some performance such as temperature and speed. It will emphasize the steering function of theory to design the screw. Although the plasticity theory is not perfect because of the limitation brought by some assumptions with heavy and complicated computation, the simulation and analysis help in understanding the behaviour of plasticity and its sensitive parameters to ease the production of specified products by using of computer tools and optimization techniques. The computer is useful for large computations and repetitive iterations. The combination of up-to-date optimization techniques and computer technology is an effective and reliable means to tackle an intractable problem.

Table 1 Plasticity trouble shooting guide with common problems and possible causes

Problems	Possible causes
Surging	High moisture content
	Die pressure too low
	Rear barrel temperature too low/too high
	Screw speed too fast
	Die land too short
	Die opening too large
	Extruder drive belt slipping
	Improper screw design
	Voltage fluctuation
	Temperature controller malfunction
	Metering depth too deep or shallow
	Warm-hot feed throat
	Material bridging in feed throat
Bubbles uniformly	High moisture content distributed through
	Melt temperature too high in extrudate
	Improper screw design (excessive shear)
	Incompatible additive
	Die temperature too high
Melt fracture	Metering depth too shallow
	Metering depth too deep
	Feed insufficient
	Die land too short
Rough surface	Improper screw design
	Incompatible additive
	Die temperature too low
	Die not streamlined
	Die land too long
	High moisture content
	Melt temperature too low
	Contamination
	Excessive output
	Regrind is not melt-compatible with virgin resin
Blocking or tacky surface	Melt temperature too high
	Die temperature too high
	Cooling take up too short
	Output excessive
	Cooling water or air too cold (polyether-type)

PHYSICAL MODEL

Generally, an injection machine includes several subsystems such as an injection system, a clamping system, a heating/cooling system, a hydraulic control system, an electricity control system, a lubricating system, a safety system and an inspecting system.

The injection component is mainly composed of

a screw and a barrel with a heater. The injection component takes in the resin and makes it melted well proportioned, and finally injects a certain amount of the melted plastic into the mould cavity with suitable speed and pressure. A favorable plasticity performance is required for the injection component. In order to model the flow of the resin in the screw, the following procedure is described.

Working status of the screw in an injection machine

The screw works with the power supplied by an electric or hydraulic motor. The movement is transmitted via a reducer from the motor. The screw rotates with a specified speed. The material in the groove is extruded to generate shearing heat by the relative movement between the screw thread and the inner wall of the barrel. When the temperature of the material reaches a certain value, the material melts. The electric heater outside the barrel maintains the barrel stand with a specified temperature.

The physical status of the resin is investigated in this paper while it is processed in the groove of a screw. This phenomenon occurs in the area shown by an ellipse in an injection machine (Fig.1). This area in Fig.1 represents the screw and the barrel to be modeled in the next paragraph. Fig.2 shows a magnified view.

Cells in the groove

In order to establish a mathematical model, the resin in the groove is presented by small cube called cell (Fig.3). N_x, N_y, N_z are layers along three directions (x, y, z) respectively, and defined by Eq.(1):

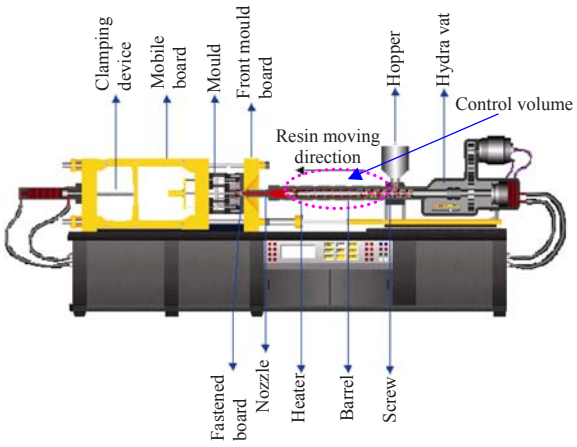

Fig.1 Injection machine

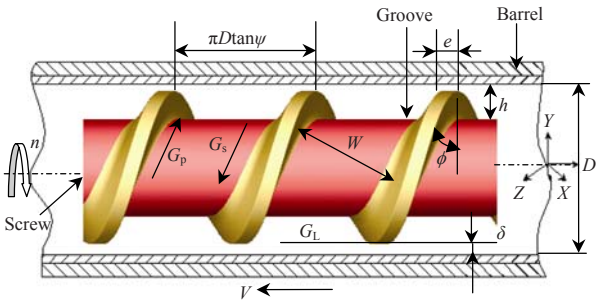

Fig.2 Screw and barrel

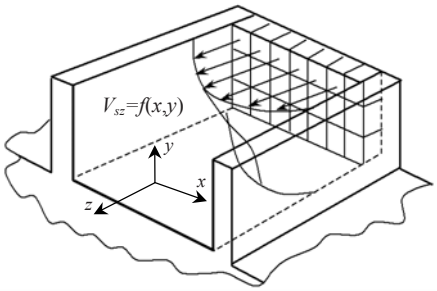

Fig.3 Physical model of the groove

$$N_x = W / L_x,\ \ N_y = H / L_y,\ \ N_z = Z / L_z, \tag{1}$$

where W is the width of groove; H is the depth of groove, Z is the length of channel, L_x, L_y, L_z are the thicknesses in x, y, z directions respectively.

The total number of the cells in the groove is given by Eq.(2):

$$N = N_x N_y N_z. \tag{2}$$

Movement and forces of a cell

Every cell in a section of the groove slips along z axis. The pressure, σ, and the frictional shearing force, τ, between the surfaces of adjacent cells are shown in Fig.4. The pressure and friction should comply with the Coulomb friction rule described by Eq.(3):

$$\tau = f\sigma, \tag{3}$$

where f is the interior frictional factor of the resin for the non-boundary cells.

However, for the boundary cells, f should be the exterior frictional coefficient between the plastic and the metal (Fig.5). To deduce the relationship between velocity and stress in a cell, an arbitrary cell (i,j) and its adjacent four cells should be analyzed.

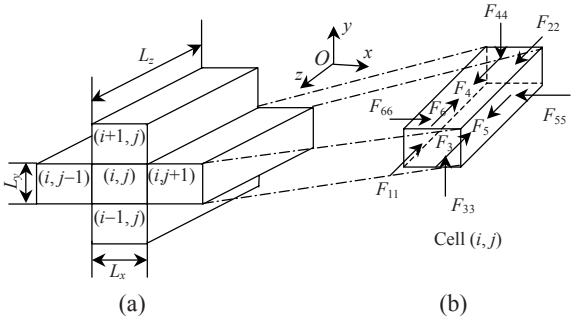

Fig.4 Adjacent cells and forces

(a) Cell (i, j) and its adjacent cells; (b) Forces applied on cell (i, j)

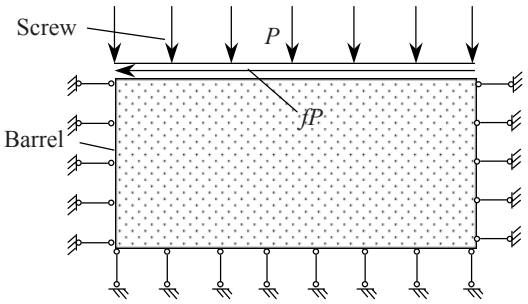

Fig.5 Force restriction on one section of the flow

Stress and strain of a cell

Although the stress distribution field in the groove is a 3D problem, the main stresses in three directions of a dispersed particle system are not independent. They hold a finite relationship between stress and strain. The relationship between stresses across and along the groove is given by Eq.(4):

$$\sigma_3 = k\sigma_z, \tag{4}$$

where k is the resin performance related coefficient; σ_3 is the stress across the groove; σ_z is the stress along the groove.

After the spatial elasticity equation is simplified, 2D elasticity equations that connect the stress and strain are obtained:

$$\{\boldsymbol{\sigma}\}=[\boldsymbol{D}]\{\boldsymbol{\varepsilon}\},\ \{\boldsymbol{\sigma}\}=\{\sigma_x,\ \sigma_y,\ \tau_{xy}\}^{\mathrm{T}},\ \{\boldsymbol{\varepsilon}\}=\{\varepsilon_x,\ \varepsilon_y,\ \dot{\gamma}_{xy}\}^{\mathrm{T}}, \tag{5}$$

where $\{\boldsymbol{\sigma}\}$ is the stress matrix for an arbitrary cell, $\{\boldsymbol{\varepsilon}\}$ is the strain matrix for an arbitrary cell, $\boldsymbol{D}$ is a 3×3 elasticity matrix for an arbitrary cell.

Relationship between velocity and stress

The elasticity energy inside a cell is ignored. According to the fictive power theory, the algebra sum of the power made in a fictive displacement by all forces applied on any body, which is in a balance status, is equal to zero (Xu and Hua, 1983):

$$\iint_A p\delta S\mathrm{d}A = 0, \tag{6}$$

where p is the force applied on the surface, which can be decomposed as the pressure stress σ and the frictional shearing force τ, δS is the displacement of a cell, A is the area of the surface.

Considering a cell (i,j) and four adjacent cells in Fig.4, cell (i,j) bears the forces along z direction (F_{11} and F_{22}), the pressure forces from adjacent cells (F_{33}, F_{44}, F_{55} and F_{66}), and the frictional shearing force (F_3, F_4, F_5 and F_6) that can be calculated by Eq.(3). So, all the forces applied to cell (i,j) are:

$$\begin{aligned}
&F_{11}=\sigma_{z(i,j)}+\Delta\sigma_{z(i,j)},\ F_{22}=\sigma_{z(i,j)},\ F_{33}=\sigma_{y(i-1,j)},\\
&F_{44}=\sigma_{y(i+1,j)},\ F_{55}=\sigma_{x(i,j+1)},\ F_{66}=\sigma_{x(i,j-1)},\\
&F_3=\tau_{(i-1,j)}=f\sigma_{y(i-1,j)},\ F_4=\tau_{(i+1,j)}=f\sigma_{y(i+1,j)},\\
&F_5=\tau_{(i,j+1)}=f\sigma_{x(i,j+1)},\ F_6=\tau_{(i,j-1)}=f\sigma_{y(i,j-1)}.
\end{aligned} \tag{7}$$

The fictive power Eq.(6) is applied to an arbitrary cell (i,j), which bears the forces expressed in Eq.(7), with awareness of the difference between the interior frictional factor and the exterior frictional factor. Then, the cell (i,j) will satisfy Eq.(8):

$$\begin{aligned}
\Delta x\Delta y\Delta\sigma_{z(i,j)}\delta S_{(i,j)}=&\Delta y\Delta z f_{(i,j+1)}(\delta S_{(i,j+1)}-\delta S_{(i,j)})\sigma_{x(i,j+1)}\\
&+\Delta y\Delta z f_{(i,j-1)}(\delta S_{(i,j-1)}-\delta S_{(i,j)})\sigma_{x(i,j-1)}\\
&+\Delta x\Delta z f_{(i+1,j)}(\delta S_{(i+1,j)}-\delta S_{(i,j)})\sigma_{y(i+1,j)}\\
&+\Delta x\Delta z f_{(i-1,j)}(\delta S_{(i-1,j)}-\delta S_{(i,j)})\sigma_{y(i-1,j)}.
\end{aligned} \tag{8}$$

If the displacement is replaced by the velocity of the cell in Eq.(8), the relationship between the velocity and the stress can be obtained as follows:

$$\begin{aligned}
&v_{(i,j)}\frac{\Delta y\Delta x}{\Delta z}(\sigma^{n+1}_{z(i,j)}-\sigma^{n}_{z(i,j)})\\
&\quad=\Delta y f^{n+1/2}_{(i,j+1)}\sigma^{n+1/2}_{x(i,j+1)}(v_{(i,j+1)}-v_{(i,j)})+
\end{aligned}$$

$$\Delta y f^{n+1/2}_{(i,j-1)}\sigma^{n+1/2}_{x(i,j-1)}(v_{(i,j-1)}-v_{(i,j)})+$$
$$\Delta x f^{n+1/2}_{(i+1,j)}\sigma^{n+1/2}_{y(i+1,j)}(v_{(i+1,j)}-v_{(i,j)})+$$
$$\Delta x f^{n+1/2}_{(i-1,j)}\sigma^{n+1/2}_{y(i-1,j)}(v_{(i-1,j)}-v_{(i,j)}),$$
$$i=1,2,...,N_x;\ j=1,2,...,N_y;\ n=1,2,...,N_z, \qquad (9)$$

where $\delta S_{(i,j)}$ is the displacement of cell located at (i, j), f is the friction coefficient, v is the velocity of cell, $v_{(i,j)}$ is velocity of cell located at (i, j), σ is the pressure stress, $\sigma^{n+1/2}_{x(i,j)}$ is the pressure stress of cell (i, j) in x direction, n is the serial number of section position in z direction, n+1/2 means the center of a cell. Δx, Δy, Δz is the cell size in x, y, z direction respectively.

From Eq.(9), it is known that the movement status of any cell is not only affected by the force from adjacent cells, but also related to the movement of adjacent cells. For each cell there are an unknown variable and its corresponding equation, i.e. the velocity and the corresponding velocity-stress coupling equation. The number of unknown variables and the number of equations are equal to form a consistent system. So, if the stress status of the cell is known, the velocity distribution can be deduced.

Solid temperature calculation

The previous calculation (Eq.(9)) encompasses velocity, relative velocity of cells, shearing and press force. Using these values, the spatial temperature distribution can be determined.

Considering the heat produced by friction between resin cells and overlooking on thermal convection in x and y directions, a 2D steady heat exchange equation that has an inner source is deduced:

$$\frac{\mathrm{d}T}{\mathrm{d}t}=a_\mathrm{s}\left(\frac{\partial^2 T}{\partial x^2}+\frac{\partial^2 T}{\partial y^2}\right)+\frac{\dot{q}}{\rho_\mathrm{s}c_\mathrm{s}}, \qquad (10)$$

where T is the temperature of the cell, $\dot{q}$ is the heat generated by friction inside the material in unit time and unit volume, a_s is the solid heat diffusivity, ρ_s is the solid density considering the interstitial space, c_s is the solid specific heat. $a_\mathrm{s}=k_\mathrm{s}/(\rho_\mathrm{s}c_\mathrm{s})$, here, k_s is the solid heat conductivity.

COMPUTATION RESULTS AND ANALYSIS

A working case is investigated from the machine shown in Fig.1. The following parameters are known and given: screw diameter=45 mm; groove width =38.38 mm; groove depth=7 mm; spire angle=17.67°; rotate speed=0.52 r/s; resin=LDPE; k=0.38; N_x=50, N_y=20, N_z=100.

Stress distribution calculation

The press force on material from the barrel is a function of the coordinates. However, in the actual calculation, the press force is worked out by an iterative method. In this method, an original distribution (e.g. uniform) of force is assumed to initiate the displacement and stress. Then, the force distribution is revised according to the displacement and stress until the following boundary conditions are satisfied:

$$u_x\geq 0 \ \text{ at } \ x=0;\ u_x\leq 0 \ \text{ at } \ x=W;$$
$$u_y\geq 0 \ \text{ at } \ y=0;\ u_y\leq 0 \ \text{ at } \ y=H,$$

where u_x, u_y are the displacements along x and y axes.

The boundary condition of the stress field is when z=0 and $\sigma_z=p_0$, where p_0 is the initial force in the feed segment of a screw.

The above calculation process is tremendously intricate and burdensome. To simplify the calculation process, the force is supposed to be of uniform distribution. In this way, the calculation load is obviously decreased, while the calculation precision holds the satisfied result. After the force distribution is obtained, the velocity distribution calculation can be launched.

Velocity distribution calculation

The combination of Eq.(9) for each cell will form a linear equation group that will be initialized and solved, then, the velocity value of each cell can be obtained.

In Fig.6a, the velocity distribution is illustrated by the height and the color of the mesh. In Fig.6b, the curve shows the velocity distribution along the width direction at particular heights. In Fig.6c, the curve shows the velocity distribution along a height direction in particular position along the width.

Temperature distribution calculation

After the differential Eq.(10) is discretised, it can be solved by iteration. Then, the temperature distribution of the material in 3D space can be obtained, as shown in Fig.7.

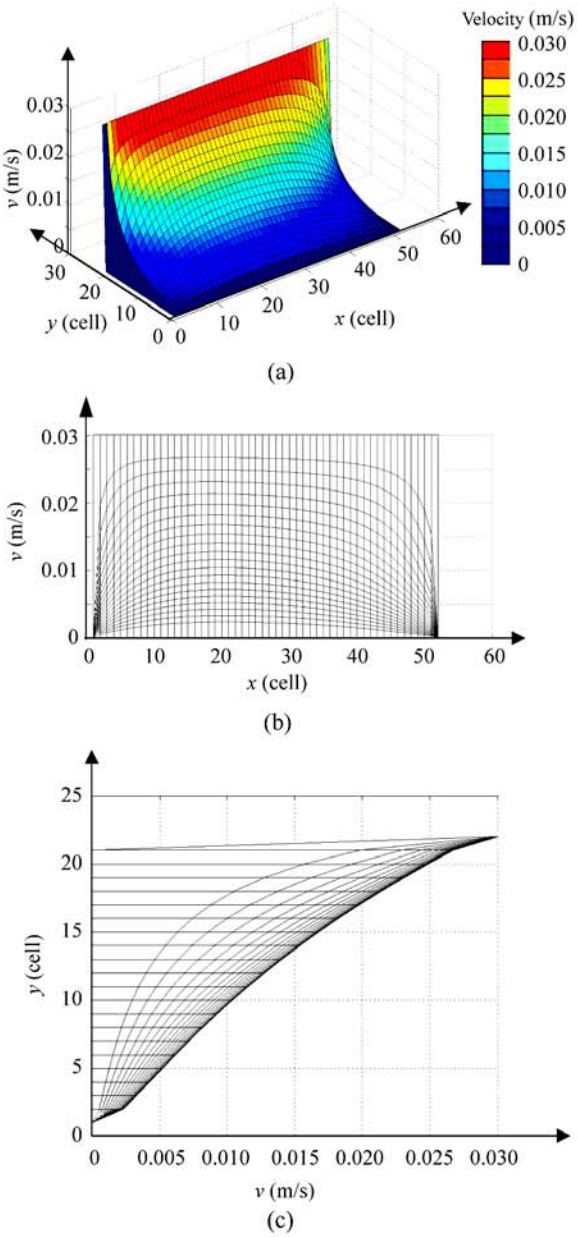

Fig.6 Velocity distribution across a section in groove
The velocity distribution illustrated (a) by the height and the color of the mesh, (b) along the width direction at particular heights and (c) along height direction in particular position along the width

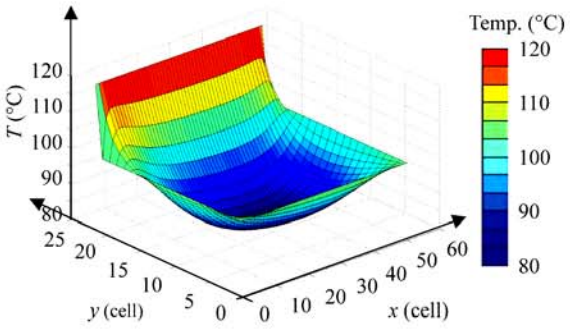

Fig.7 Temperature distribution of a section near entrance

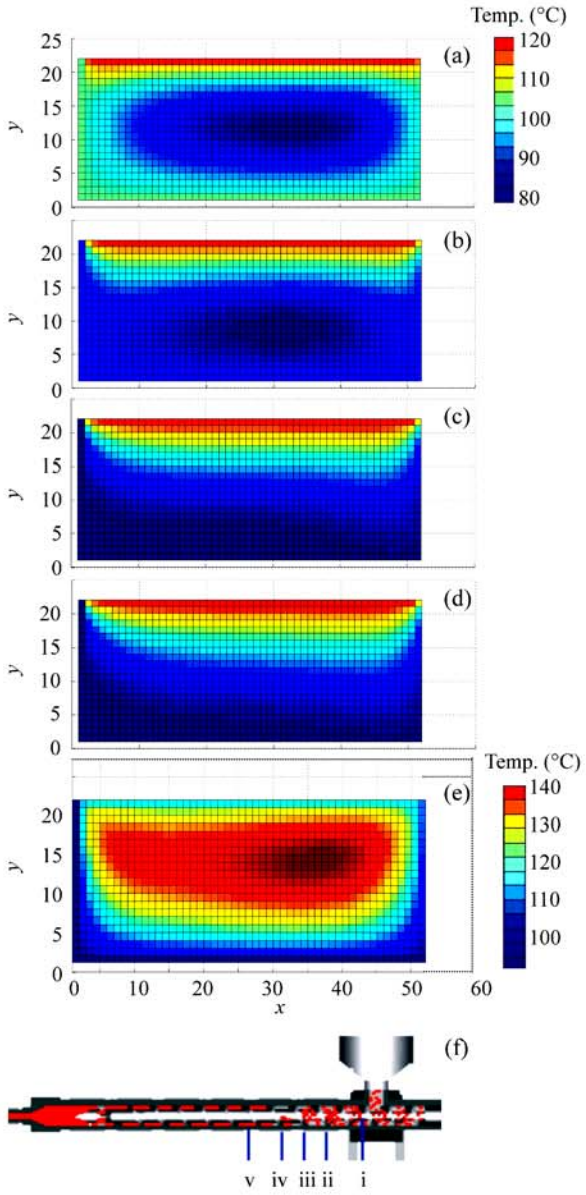

Fig.8 Temperature distribution of a section away from entrance gradually
(a)~(e) denote the temperature distribution of sections located on positions i~v in control volumn (f), respectively

Fig.8 shows the distribution of the temperature across several sections, e.g., cells along the flow. At the beginning, the higher temperature is located on top of the sections, i.e., area where embedded heaters are implemented outside the barrel. Figs.8a~8e represent temperature distribution of sections of the material from its entrance. As a result of the boundary condition control, the temperature of four margins of

every section remains the same. Furthermore, the upper side of the section has the value of the barrel temperature (e.g., 120 °C), while the other three sides have the value of the screw temperature (e.g., 100 °C).

It can be seen from Fig.8 that the temperature distribution is changing along the flow at different sections. At the beginning, the temperature of the material in the center of the groove is low, and it is lower than the temperature of the barrel or the screw. As the material is conveyed forward, the iterative calculation is carried out. Then, the temperature of the material in some area of the groove will increase because of the heat generated by shear stress. At a particular position, the temperature of the material in the center of the groove becomes higher than that of the barrel or the screw. And, unexpected case may occur when the temperature of resin material exceeds its decomposing temperature.

CONCLUSION

The analysis of the resin behavior in the screw with particular emphasis on the temperature and velocity has been carried out by using numerical simulation of the injection process. The mathematical modeling of the behaviour with the previous parameters has led to the following conclusions:

(1) The plasticity is a combined result of the resin performance, screw structure and process parameter.

(2) The highest temperature appears in the center of the groove rather than in the margin of groove.

(3) The melted resin will see its speed increasing in a laminar shape.

(4) The control of process parameters such as the heating temperature and speed of screw will help in improving the quality of the product.

(5) The process modeling could lead to a redesign of the screw to suit specific requirements.

References

Bogaerds, A.C.B., Verbeeten, W.M.H., Peters, G.W.M., Baaijens, F.P.T., 1999. 3D Viscoelastic analysis of a polymer solution in a complex flow. *Computer Methods in Applied Mechanics and Engineering*, **180**(3-4):413-430. [doi:10.1016/S0045-7825(99)00176-0]

Bogaerds, A.C.B., Hulsen, M.A., Peters, G.W.M., Baaijens, F.P.T., 2004. Stability analysis of injection molding flows. *Journal of Rheology*, **48**(4):765-785. [doi:10.1122/1.1753276]

Cheung, A., Yu, Y., Pochiraju, K., 2004. Three-dimensional finite element simulation of curing of polymer composites. *Finite Elements in Analysis and Design*, **40**(8):895-912. [doi:10.1016/S0168-874X(03)00119-7]

Das, C., Inkson, N.J., Read, D.J., Kelmanson, M.A., McLeish, T.C.B., 2006. Computational linear rheology of general branch-on-branch polymers. *Journal of Rheology*, **50**(2):207-234. [doi:10.1122/1.2167487]

Ekh, J., Schön, J., 2008. Finite element modeling and optimization of load transfer in multi-fastener joints using structural elements. *Composite Structures*, **82**(2):245-256. [doi:10.1016/j.compstruct.2007.01.005]

Ghoreishy, M.H.R., Razavi-Nouri, M., Naderi, G., 2005. Finite element analysis of a thermoplastic elastomer melt flow in the metering region of a single screw extruder. *Computational Materials Science*, **34**(4):389-396. [doi:10.1016/j.commatsci.2005.01.011]

Hasanpour, K., Ziaei-Rad, S., 2007. Finite Stain Viscoelastic-plastic Deformation of Polymers Using Finite Element Simulation. Proceedings of the 9th International Conference on Numerical Methods in Industrial Forming Processes, p.1301-1306.

Kessels, J.F.A., Jonker, A.S., Akkerman, R., 2007. Fully 2½D flow modeling of resin infusion under flexible tooling using unstructured meshes and wet and dry compaction properties. *Composites Part A: Applied Science and Manufacturing*, **38**:51-60. [doi:10.1016/j.compositesa.2006.01.025]

Lerdwijitjarud, W., Sinvat, A., Larson, R.G., 2004. Influence of dispersed-phase elasticity on steady-state deformation and breakup of droplets in simple shearing flow of immiscible polymer blends. *Journal of Rheology*, **48**(4):843-862. [doi:10.1122/1.1753275]

Lesniak, D., Libura, W., 2007. Extrusion of sections with varying thickness through pocket dies. *Journal of Materials Processing Technology*, **194**(1-3):38-45. [doi:10.1016/j.jmatprotec.2007.03.123]

Mackerle, J., 2003. Finite element analysis and simulation of polymers—an addendum: a bibliography (1996-2002). *Modelling and Simulation in Materials Science and Engineering*, **11**(2):195-231. [doi:10.1088/0965-0393/11/2/307]

Restrepo, O., Hsiao, K.T., Rodriguez, A., Minaie, B., 2007. Development of adaptive injection flow rate and pressure control algorithms for resin transfer molding. *Composites Part A: Applied Science and Manufacturing*, **38**(6):1547-1568. [doi:10.1016/j.compositesa.2007.01.005]

Russo, A., Zuccarello, B., 2007. Experimental and numerical evaluation of the mechanical behaviour of GFRP sandwich panels. *Composite Structures*, **81**(4):575-586. [doi:10.1016/j.compstruct.2006.10.007]

Savarmand, S., Heniche, M., Béchard, V., Bertrand, F., Carreau, P.J., 2007. Analysis of the vane rheometer using 3D finite element simulation. *Journal of Rheology*, **51**(2):161-177.

[doi:10.1122/1.2433936]

Shojaei, A., 2006. Numerical simulation of three-dimensional flow and analysis of filling process in compression resin transfer moulding. *Composites Part A: Applied Science and Manufacturing*, **37**(9):1434-1450. [doi:10.1016/j.compositesa.2005.06.021]

Shojaei, A., Ghaarian, S.R., Karimian, S.M., 2004. Three-dimensional process cycle simulation of composite parts manufactured by resin transfer molding. *Composite Structures*, **65**(3-4):381-390. [doi:10.1016/j.compstruct.2003.12.001]

Wilczyñski, K., 2001. SSEM: a computer model for a polymer single-screw extrusion. *Journal of Materials Processing Technology*, **109**(3):308-313. [doi:10.1016/S0924-0136(00)00821-9]

Wilczyñski, K., Tyszkiewicz, A., Szymaniak, Z., 2001. Modeling for morphology development during single-screw extrusion of LDPE/PS blend. *Journal of Materials Processing Technology*, **109**(3):320-323. [doi:10.1016/S0924-0136(00)00820-7]

Xu, C.D., Hua, B.H., 1983. The Theory, Method and Programs of the Mechanics Finite Element. Waterpower Publishing Company, Beijing, p.33-36 (in Chinese).

Zampaloni, M., Pourboghrat, F., Yankovich, S.A., Rodgers, B.N., Moore, J., Drzal, L.T., Mohanty, A.K., Misra, M., 2007. Kenaf natural fiber reinforced polypropylene composites: A discussion on manufacturing problems and solutions. *Composites Part A: Applied Science and Manufacturing*, **38**(6):1569-1580. [doi:10.1016/j.compositesa.2007.01.001]